Ab Initio Molecular Orbital and Density Functional Theoritical Studies on 1-Naphtol

G. Raja, K. Saravanan, and S. Sivakumar

***Abstract*—The molecular vibrations of 1-Naphtol were investigated in polycrystalline sample, at room temperature, by FT- IR and FT-Raman spectroscopy. In parallel, ab initio and various density functional (DFT) methods were used to determine the geometrical, energetic and vibrational characteristics of 1-Naphtol . On the basis of B3LYP/6-31G* and B3LYP/6-311+G** methods and basis set combinations, a normal mode analysis was performed to assign the various fundamental frequencies according to the total energy distribution (TED). The vibrational spectra were interpreted, with the aid of normal coordinate analysis based on a scaled quantum mechanical force field. The Infrared and Raman spectra were also predicted from the calculated intensities. Comparison of simulated spectra with the experimental spectra provides important information about the ability of the computational method to describe the vibrational modes. Simulation of Infrared and Raman spectra, utilizing the results of these calculations led to excellent overall agreement with observed spectral patterns. The investigation is performed using quantum chemical calculations conducted by means of the Gaussian 98W and Guassview set of programs. Further, density functional theory (DFT) combined with quantum chemical calculations to determine the first-order hyperpolarizability.**

***Index Terms*—Vibrational spectra; fourier transform infrared and FT-raman spectra; DFT calculation, first-order hyperpolarizability**

I. Introduction

1-Naphthol and derivatives thereof can also be used for the preparation of chiral ligands as contemplated by the present disclosure. Yet further naphthol derivatives are known in the art and are within the capacity of a skilled technician. 1-naphthol has been frequently used in chemical industries, e.g., in production of dyes, plastics, synthetic rubber, plant protecting formulations, etc. The toxicity of 1-naphthol is considered similar to that of naphthalene and carbaryl. Due to the presence of a hydroxyl group in its molecular structure,1-naphthol solubility in water as well as its mobility in natural aquifers is enhanced.

Biological monitoring is the best way for assessing exposure to organic contaminants and involves the measurement of a biomarker of exposure (usually the contaminant or a metabolite) in human blood, urine or biological tissues.

So, fast, accurate and sensitive analytical methods are necessary for the examination of human exposure. 1-naphthol is an urinary metabolite of both naphthalene and carbaryl. As the biological half-live of carbaryl is on the order of days, 1-naphthol is an urinary biomarker of exposure to carbaryl indicative only of recent exposure.

Accurate vibrational assignment for aromatic and another conjugated system is necessary for characterization of materials. Assignment for complex systems can be proposed on the basis of frequency agreement between the computed harmonics and the observed fundamentals. Quantum chemical computational methods have proven to be an essential tool for interpreting and predicting vibrational spectra [1-2]. A significant advance in this area was made by scaled quantum mechanical (SQM) force field method [3-6]. In the SQM approach the systematic errors of the computed harmonic force field are corrected by a few scale factors which were found to be well transferable between chemically related molecules [2,7–9]. Recent spectroscopic studies on these materials have been motivated because the vibrational spectra are very useful for the understanding of specific biological process and in the analysis of relatively complex systems.

In the present study, we extend a probing into the application of the B3LYP/6-31G* (small basis set) and B3LYP/6-311+G** (large basis set) based on SQM method [2] to vibrational analysis and conformational stability of 1-Naphtol. The main difficulty in such investigation is that the vibrational spectra of these compounds have not been completely analyzed until now and generally only rough assignments are available. The geometrical parameters of the most optimized geometry obtained via energy calculations were used for the DFT calculations. The infrared and Raman intensities were also predicted. Based on these calculations, the simulated FT-IR and FT-Raman spectra were obtained. The observed and the simulated spectra agrees well.

II. Materials and Methods

A. Experimental Details

The fine polycrystalline samples of 1-Naphtol were obtained from the Lancaster chemical company, UK, and used as such for the spectral measurements. The room temperature Fourier transform infrared spectra of the title compounds were measured in the 4000–400 cm^{-1} region at a resolution ±1cm^{-1} using KBr pellets on Perkin-Elmer RX1

Manuscript received June 13, 2011; recised September 2, 2011..

G.Raja is with the department of Chemistry, Paavai Engineering College, Namakkal-637 018, India. (genuineraja@gmail.com)

K.Saravanan is with the department of Chemistry, Thiruvalluvar Government Arts College, Rasipuram-637 401, India. (npksaran@yahoo. co.in)

S.Sivakumar is with the department of Physics, Arignar Anna Government Arts College, Attur-636 121, India. (photonic_ss@rediffmail. com)

FT-IR spectrophotometer equipped with He–Ne laser source, KBr beam splitter and LiTaO3 detector. Boxcar apodisation was used for the 250 averaged interferograms collected for both the samples and background. The FT-Raman spectra of 1-Naphtol were recorded on a BRUKERIFS-66V model interferometer equipped with an FRA106 and a FT-Raman accessory. The spectra were recorded in the 3500–100 cm^{-1} stokes region using the 1064 nm line of a Nd:YAG laser for the excitation operating at 200mW power. The reported wave numbers are believed to be accurate within ±1 cm^{-1}.

B. Computational Details

The calculation of the vibrational frequencies is essential and also useful for the vibrational assignments of the spectra. Quantum chemical calculations for 1-Naphtol was performed with the Gaussian 98W program [10] using the Becke 3-Lee-Yang-Parr (B3LYP) functional [11,12] supplemented with the standard B3LYP/6-31G* (small basis set) and B3LYP/6-311+G** (large basis set) for the Cartesian representation of the theoretical force constants have been computed at the fully optimized geometry by assuming *C*s point group symmetry. Scaling of the force field was performed according to the SQM procedure [13,14] using selective (multiple) scaling in the natural internal coordinate representation[15,16]. Transformations of the force field and the subsequent normal coordinate analysis including the least squares refinement of the scaling factors, calculation of total energy distribution (TED) and IR and Raman intensities were done on a PC with the MOLVIB program (Version V7.0-G77) written by Sundius[17,18]. The TED elements provide a measure of each internal coordinates contribution to the normal coordinate. For the plots of simulated IR and Raman spectra, pure Lorentzian band shapes were used with a bandwidth of 10 cm^{-1}.The prediction of Raman intensities was carried out by following the procedure outlined below. The Raman activities calculated by the Gaussian 98W program and adjusted during scaling procedure with MOLVIB were converted to relative Raman intensities using the following relationship derived from the basic theory of Raman scattering [19-21].

$$I_i = \frac{f(v_o - v_i)^4 S_i}{v_i[1 - \exp(-hcv_i / kT)]}$$

where v_o is the exciting frequency (in cm^{-1} units), v_i the vibrational wavenumber of the i^{th} normal mode, h, c and k are the universal constants and f is the suitably chosen common scaling factor for all the peak intensities.

C. First-order hyperpolarizability calculations

The nonlinear response of an isolated molecule in an electric field $E_i(\omega)$ can be represented as a Taylor expansion of the total dipole moment μ_t induced by the field:

$$\mu_t = \mu_0 + \alpha_{ij}E_i + \beta_{ijk}E_iE_j + ...$$

where α is linear polarizability, μ_0 the permanent dipole moment and β_{ijk} are the first-order hyperpolarizability tensor components.

The components of first-order hyperpolarizability can be determined using the relation

$$\beta_i = \beta_{iii} + \frac{1}{3}\sum_{i \neq j}(\beta_{ijj} + \beta_{jij} + \beta_{jji})$$

Using the x, y and z components the magnitude of the total static dipole moment (μ), isotropic polarizability (α_0), first-order hyperpolarizability (β_{total}) tensor, can be calculated by the following equations:

$$\mu_1^0 = (\mu_x^2 + \mu_y^2 + \mu_z^2)^{1/2}$$

$$\beta_{tot} = (\beta_x^2 + \beta_y^2 + \beta_z^2)^{1/2}$$

The complete equation for calculating the first-order hyperpolarizability from Gaussian 98W output is given as follows [10]:

$$\beta_{tot} = [(\beta_{xxx} + \beta_{xyy} + \beta_{xzz})^2 + (\beta_{yyy} + \beta_{yzz} + \beta_{yxx})^2 + (\beta_{zzz} + \beta_{zxx} + \beta_{zyy})^2$$

The β components of GAUSSIAN 98W output are reported in atomic units, the calculated values have to be converted into electrostatic units (1 a.u= 8.3693 $x10^{-33}$ esu)..

Before calculating the hyperpolarizability for the investigated compound, the optimization has been carried out in the UHF (unrestricted open-shell Hartree-Fock) level. Molecular geometries were fully optimized by Berny's optimization algorithm using redundant internal coordinates. All optimized structures were confirmed to be minimum energy conformations.

An optimization is complete when it has converged. i.e., when it has reached a minimum on the potential energy surface, thereby predicting the equilibrium structures of the molecules. This criterion is very important in geometry optimization. The inclusion of d polarization and double zeta function in the split valence basis set is expected to produce a marked improvement in the calculated geometry [22]. At the optimized structure, no imaginary frequency modes were obtained proving that a true minimum on the potential energy surface was found. The electric dipole moment and dispersion free first-order hyperpolarizibility were calculated using finite field method. The finite field method offers a straight forward approach to the calculation of hyperpolarizabilities [23]. All the calculations were carried out at the DFT level using the three-parameter hybrid density functional B3LYP and a 3-21 G (d, p) basis set.

III. Results and Discussion

A. Molecular geometry

The optimized molecular structure of 1-Naphtol was shown in Fig.1. The global minimum energy obtained by the DFT structure optimization was presented in Table I. The optimized geometrical parameters obtained by the large basis set calculation were presented in Table II.

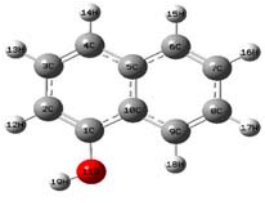

Fig. 1.The optimized molecular structure of 1-Naphtol

TABLE I: TOTAL ENERGIES OF 1-NAPHTOL , CALCULATED AT DFT (B3LYP)/6-31G* AND (B3LYP)/6-311+G** LEVEL

Method	Energies (Hartrees)
6-31G*	-461.084753
6-311+G**	-461.109185

Detailed description of vibrational modes can be given by means of normal coordinate analysis (NCA). For this purpose, the full set of 72 standard internal coordinates containing 21 redundancies were defined as given in Table 3. From these, a non-redundant set of local symmetry coordinates were constructed by suitable linear combinations of internal coordinates following the recommendations of Fogarasi et. al [15, 16] are summarized in Table 4. The theoretically calculated DFT force fields were transformed in this later set of vibrational coordinates and used in all subsequent calculations.

B. Analysis of vibrations spectra

The 51 normal modes of 1-Naphtol are distributed among the symmetry species as Γ_{3N-6}= 35 A' (in-plane) + 16 A″ (out-of-plane), and in agreement with C_s symmetry.

All the vibrations were active both in Raman scattering and infrared absorption. In the Raman spectrum the in-plane vibrations (A') give rise to polarized bands while the out-of-plane ones (A″) to depolarized band. The TED were reported in Table 5.For visual comparison, the observed and simulated FT-IR and FT-Raman spectra of 1-Naphtol are produced in a common frequency scales in Fig. 2 & Fig. 3.Root mean square (RMS) values of frequencies were obtained in the study using the following expression,

$$RMS = \sqrt{\frac{1}{n-1}\sum_{i}^{n}\left(\upsilon_i^{calc} - \upsilon_i^{exp}\right)^2}$$

The RMS error of the observed and calculated frequencies (unscaled / B3LYP/6-311+G**) of 1-Naphtol was found to be 107 cm^{-1}. This is quite obvious; since the frequencies calculated on the basis of quantum mechanical force fields usually differ appreciably from observed frequencies. This is partly due to the neglect of an harmonicity and partly due to the approximate nature of the quantum mechanical methods.In order to reduce the overall deviation between the unscaled and observed fundamental frequencies, scale factors were applied in the normal coordinate analysis and the subsequent least square fit refinement algorithm resulted into a very close agreement between the observed fundamentals and the scaled frequencies.Refinement of the scaling factors applied in this study achieved a weighted mean deviation of 9 cm^{-1} between the experimental and scaled frequencies of the title compound.

C-C vibrations:

The bands between 1480 and 1650 cm^{-1} are assigned to C-C stretching modes [24]. In the present study, the carbon stretching vibrations of the title compound have been observed at 1572,1636 cm^{-1} in the FT-IR and 1572 cm^{-1} in FT-Raman spectrum. These assignments are in good agreement with literature [25,26]. In present investigation, the C-C mode mixes with C–H in-plane bending vibrations.

TABLE II: OPTIMIZED GEOMETRICAL PARAMETERS OF 1-NAPTHOL OBTAINED BY B3LYP/ 6–311+G** DENSITY FUNCTIONAL CALCULATIONS

Bond length	Value(Å)	Bond angle	Value(Å)	Dihedral angle	Value(Å)
C2-C1	1.379	C3-C2-C1	120.157	C4-C3-C2-C1	-0.013
C3-C2	1.414	C4-C3-C2	120.797	C5-C4-C3-C2	0.022
C4-C3	1.375	C5-C4-C3	120.255	C6-C5-C4-C3	-179.976
C5-C4	1.421	C6-C5-C4	122.131	C7-C6-C5-C4	-179.955
C6-C5	1.420	C7-C6-C5	121.089	C8-C7-C6-C5	0.048
C7-C6	1.376	C8-C7-C6	120.320	C9-C8-C7-C6	-0.092
C8-C7	1.415	C9-C8-C7	120.296	C10-C9-C8-C7	0.054
C9-C8	1.377	C10-C9-C8	120468	O11-C1-C2-C3	179.945
C10-C9	1.418	O11-C1-C2	122.792	H12-C2-C3-C4	179.953
O11-C1	1.368	H12-C2-C3	119.938	H13-C3-C4-C5	-179.963
H12-C2	1.088	H13-C3-C4	120.253	H14-C4-C5-C6	0.0186
H13-C3	1.086	H14-C4-C5	119.064	H15-C6-C7-C8	-179.981
H14-C4	1.086	H15-C6-C7	120.364	H16-C7-C8-C9	179.952
H15-C6	1.087	H16-C7-C8	119.674	H17-C8-C9-C10	-179.985
H16-C7	1.086	H17-C8-C9	119.985	H18-C9-C10-C1	0.086
H17-C8	1.086	H18-C9-C10	118.791	H19-O11-C1-C2	-0.096
H18-C9	1.084	H19-O11-C1	108.727		
H19-O11	0.969				

*for numbering of atom refer Fig. 1

C-H vibrations:

The presence of hetero-aromatic-type structure is best recognized by the presence of C–H stretching vibrations [27] near 3030 cm^{-1}. Aromatic compounds commonly exhibit multiple weak bands in the region 3100–3000 cm^{-1} due to aromatic C–H stretching vibrations. The bands due to C–H in-plane ring bending vibration interacting with C–C stretching vibration are observed as a number of m-w intensity sharp bands in the region 1300–1000 cm^{-1}. C–H out-of-plane bending vibrations are strongly coupled vibrations and occur in the region 900–667 cm^{-1}. Accordingly, in the present study the C–H vibrations of the title compounds are observed at 3177, 3186 cm^{-1} in the FT-IR spectrum and 3166 in FT-Raman for 1-Naphtol .

C-O vibrations:

The non-linearity of hydrogen bond in 1-Naphtol have an impact over the carbonyl group frequency. The interaction of carbonyl group with the other group present in the system does not produce such a drastic and characteristic changes in the frequency of C O stretch.

TABLE III: DEFINITION OF INTERNAL COORDINATES OF 1-NAPTHOL

No(i)	symbol	Type	Definition
Streching 1 -7	r_i	C-H	C2-H11,C3-H13,C4-H14,C6-H15, C7-H16,C8-H17,C9-H18
8	q_i	C-O	C1-O11
9	Q_i	O-H	O11-H19
10-20	R_i	C-C	C1-C2,C2-C3,C3-C4,C4-C5, C5-C6,C6-C7,C7-C8,C8-C9, C9-C10,C10-C1,C10-C5
Bending 21-34	β_i	C-C-H	C1-C2-H12,C3-C2-H12,C2-C3-H13.C4-C3-H13,C3-C4-H14,C5-C4-H14, C5-C6-H15, C7-C6-H15, C6-C7-H16, C8-C7-H16, C7-C8-H17, C9-C8-H17, C8-C9-H18, C10-C9-H18.
35-36	θ_i	C-C-O	C10-C1-O11,C2-C1-O11
37	ϕ_i	C-O-H	C1-O11-H19
38-43	α_i	bring1	C1-C2-C3, C2-C3-C4,C3-C4-C5, C4-C5-C10,C5-C10-C5,C10-C1-C2
44-49	α_i	bring2	C5-C6-C7,C6-C7-C8,C7-C8-C9, C8-C9-C10,C9-C10-C5,C10-C5-C6
Out-of-plane bending 50-56	ω_i	ωC-H	H12-C2-C1-C3,H13-C3-C2-C4, H14-C4-C3-C5,H15-C6-C5-C7, H16-C7-C6-C8,H17-C8-C7-C9, H18-C9-C8-C10.
57	ω_i	ωC-O	O11-C1-C10-C2
Torison 58-63	τ_i	tring1	C1-C2-C3-C4,C2-C3-C4-C5, C3-C4-C5-C10,C4-C5-C10-C1, C5-C10-C1-C2,C10-C1-C2-C3
64-69	τ_i	tring2	C5-C6-C7-C8,C6-C7-C8-C9, C7-C8-C9-C10,C8-C9-C10-C5, C9-C10-C5-C6,C10-C5-C6-C7
70	τ_i	τO-H	C2(C10)-C1-O11-H19
71-72	τ_i	Butterfly	C4-C5-C10-C9,C6-C5-C10-C1

*for numbering of atom refer Fig. 1

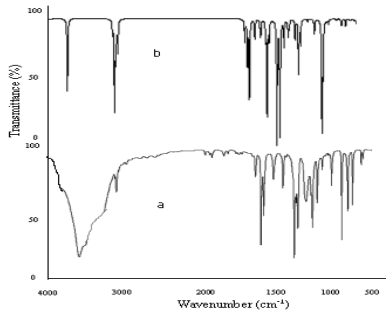

Fig. 2.FT-IR spectra of 1-Naphtol .
(a) Observed (b) Calculated with B3LYP/6-311+G**

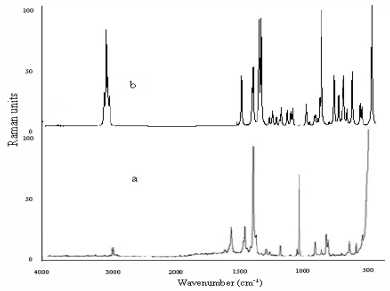

Fig. 3.FT-Raman spectra of 1-Naphtol .
(a) Observed (b) Calculated with B3LYP/6-311+G**

The carbonyl stretching frequency is very sensitive to the factors that disturb the nature of the carbonyl group and its precise frequency is characteristic of the type of the carbonyl compound being studied. Particularly detailed correlations have been made for the carbonyl bond stretching frequency.The carbonyl stretching frequency has been most extensively studied by infrared spectroscopy. This multiply bonded group is highly polar ($>C^{\delta+}=O^{\delta-}$) and therefore gives rise to an intense infrared absorption band.

The carbon-oxygen double bond is formed by the p_π–p_π bonding between carbon and oxygen. Because of the different electro-negativities of carbon and oxygen atoms, the bonding electrons are not equally distributed between the two atoms. The following two resonance forms contribute to the bonding of the carbonyl group $>C=O \leftrightarrow C^{+}\text{-}O^{-}$. The lone pair of electrons on oxygen also determines the nature of the carbonyl group. The position of the C=O stretching vibration is very sensitive to various factors such as the physical state, electronic effects by substituents, ring strains, etc. [24].

Consideration of these factors provides further information about the environment of the C=O group. The carbonyl stretching generally occurs as a strong absorption in the region from 1730 to 1645 cm^{-1}.

This portion of the infrared spectrum is most useful because the position of the carbonyl absorption is quite sensitive to substitution effects and the geometry of the molecule. Accordingly, in the present investigation, the peaks identified at 1810 cm^{-1} have been assigned to C=O stretching vibrations for 1-Naphtol .

O-H vibrations

The precise positions of O–H band are dependent on the strength of hydrogen bond. The O–H stretching appears at 3590–3400 cm^{-1} in the inter-molecular hydrogen bonded systems. The observed peaks in this region are sharp and strong. The title compounds in this study showed a very strong absorption peak at 3753 cm^{-1} which are due to the O–H stretching vibrations.

C–O stretching and O–H bending vibrations

Two bands arising from C–O stretching and O–H bending appear in the spectra of carboxylic acids near 1210–1320 and 1400–1440 cm^{-1}, respectively. Both these bands involve some interaction between C–O stretching and in- plane

C–O–H bending. The more intense band near 1280–1315 cm^{-1} for dimers is generally referred to as C-O stretching band and it usually occurs as a doublet in the spectra of long-chain fatty acids. One of the characteristic bands in the spectra of dimeric carboxylic acid arises from the out-of-plane bending of the hydrogen bonded OH. It appears near 1070 cm^{-1} and is characteristically broad with medium intensity [24].

TABLE IV: DEFINITON OF LOCAL SYMMETRY COORDINATES AND THE VALUE CORRESPONDING SCALE FACTORS USED TO CORRECT THE FORCE FIELDS FOR 1-NAPTHOL

No.(i)	Symbol[a]	Definition[b]
1-7	C-H	r1,r2,r3,r4,r5,r6,r7
8	C-O	q8
9	O-H	Q9
10-20	C-C	R10,R11,R12,R13,R14,R15,R16,R17,R18,R19,R20
21-27	C-C-H	(β21- β22) /√2,(β23- β24) /√2,(β25- β 26) /√2 (β27- β 28) /√2, (β29- β 30) /√2,(β31- β32) /√2, (β33- β34) /√2
28	C-C-O	(θ35-θ36) /√2
29	C-O-H	ϕ37
30	bring1	(α38-α39+α40-α41+α42-α43)/ √6
31	bring1	(2α38-α39-α40+2α41-α42-α43) √12
32	bring1	(α39-α40+α42-α43)/2
33	bring2	(α44-α45+α46-α47+α48-α49)/ √6
34	bring2	(2α44-α45-α46+2α47-α48-α49) √12
35	bring2	(α45-α46+α48-α49)/2
36-42	ωC-H	ω50, ω51, ω52, ω53, ω54, ω55, ω56
43	ωC-O	ω57
44	tring1	(τ58-τ59+τ60-τ61+τ62-τ63) √6
45	tring1	(τ58-τ60+τ61-τ63)/2
46	tring1	(-τ58+2τ59-τ60-τ61+2τ62-τ63) √12
47	tring2	(τ64-τ65+τ66-τ67+τ68-τ69) √6
48	tring2	(τ64-τ65+τ66-τ67)/2
49	tring2	(-τ64+2τ65-τ66-τ67+2τ68-τ69) √12
50	τO-H	τ70
51	Butterfly	(τ71-τ72) /√2

[a] These symbols are used for description of the normal modes by TED in Table V.
[b] The internal coordinates used here are defined in Table 3.

TABLE V: THE TOTAL ENERGY DISTRIBUTION OF 1-NAPTHOL

Frequency (cm^{-1})	Total Energy Distribution
143	tring1(60),tring2(31),gCH (7)
177	tCC(28),tring1(25),tring2(25),gCH(16),gCO(6)
265	tring1(45),tring2(21),gCH(15),tCC(11),gCO(7)
284	bCO (38),bring2(25),bring1(21),CC(14)
367	tOH(85),tring2(10)
433	tring2(57),gCH(16),tCC(10),gCO(9),tring1(5)
469	bCO(38),CC(25),bring1(19),bring2(14)
479	tring1(42),tring2(40),gCH(15)
487	bring1(59),bring2(24),CC(11)
532	bring1(34),bring2(30),bCO(19),CC(13)
584	bring2(49),bring1(24),CC(16)
585	tring1(42),gCH(19),tring2(14),tCC(13),gCO(12)
645	tring2(33),gCO(26),tring1(26),gCH(14)
726	CC(48),bring2(31),bring1(8),CO(8)
745	gCH(74),tring2(19),tring1(7)
788	gCH(60),tring2(16),tring1(15),gCO(6)
801	bring1(40),bring2(33),CC(23)
803	gCH(40),tring1(31),tring2(20),gCO(9)
853	gCH(81),tring1(11),gCO(7)
888	gCH(75),tring2(14),tring1(10)
891	bring1(34),bring2(33),CC(20),CO(7)
954	gCH(92),tring1(6)
963	gCH(90)
991	gCH(87),tring2(13)
1049	CC(74),bCH(14)
1070	CC(37),bring2(19),bCH(16),CO(10),bring1(8)
1110	CC(45),bCH(27),bring2(17),CO(8)
1176	bCH(52),CC(33),bring1(8),bOH(6)
1186	bCH(59),CC(35),bOH(5)
1197	bCH(76),CC(14)
1233	CC(48),bCH(31),bOH(19)
1269	CC(33),bOH(28),bCH(25),bring2(12)
1281	bCH(52),CC(28),bring1(7),CO(6)
1318	bCH(36),CO(27),CC(21),bring1(15)
1406	CC(78),bCH(13)
1428	CC(78),bCH(12)
1448	bCH(60),CC(25),bring1(6),CO(6)
1505	bCH(59),CC(33)
1514	bCH(44),CC(41)
1572	CC(57),bCH(32)
1636	CC(70),bCH(13),bring1(8),bring2(6)
1658	CC(68),bCH(23)
1689	CC(66),bCH(13),bring1(9),bring2(8)
3166	CH(99)
3177	CH(99)
3186	CH(99)
3190	CH(99)
3203	CH(99)
3205	CH(99)
3227	CH(99)
3753	OH(100)

Ring vibrations:

Several ring modes are affected by the substitution in the aromatic ring. In the present study, the bands absorbed at 1110, 1176 cm^{-1} and 479,585 cm^{-1} have been designated to ring in-plane and out-of-plane bending modes, respectively. For most of the remaining ring vibrations, the overall agreement is satisfactory. Small changes in frequencies observed for these modes are due to the changes in force constants/reduced mass ratio resulting mainly due to the extent of mixing between ring and substituent group.

IV. HYPERPOLARIZABILITY CALCULATIONS

The first-order hyperpolarizibility (β_{ijk}) of the novel molecular system of 1-Naphtol is calculated using 3-21 G (d,p) basis set based on finite field approach. Hyperpolarizibility is a third rank tensor that can be described by a 3 x 3 x 3 matrix. It strongly depends on the method and basis set used. The 27 components of 3D matrix can be reduced to 10 components due to Kleinman symmetry[27].The calculated first-order hyperpolarizability (β_{total}) of 1-Naphtol is 1.1070×10^{-30} esu, which is nearly seven times that of urea (0.1947×10^{-30} esu). The calculated dipole moment (μ) and first-order hyperpolarizibility (β) are shown in Table VI.

The theoretical calculation seems to be more helpful in determination of particular components of β tensor than in establishing the real values of β. Domination of particular components indicates on a substantial delocalization of charges in those directions. It is noticed that in β_{xxx} (which is the principal dipole moment axis and it is parallel to the charge transfer axis) direction, the biggest values of hyperpolarizability are noticed and subsequently

delocalization of electron cloud is more in that direction. The higher dipole moment values are associated, in general, with even larger projection of β_{total} quantities. The electric dipoles may enhance, oppose or at least bring the dipoles out of the required net alignment necessary for NLO properties such as β_{total} values. The connection between the electric dipole moments of an organic molecule having donor–acceptor substituent and first hyperpolarizability is widely recognized in the literature [28,29]. The maximum β was due to the behavior of non-zero μ value. One of the conclusions obtained from this work is that non-zero μ value may enable the finding of a non-zero β value. Of course Hartee–Fock calculations depend on the mathematical method and basis set used for a polyatomic molecule.

TABLE VI: THE DIPOLE MOMENT (μ) AND FIRST-ORDER HYPERPOLARIZIBILITY (β) OF 1-NAPHTOL DERIVED FROM DFT CALCULATIONS

β_{xxx}	-30.036823
β_{xxy}	30.0437602
β_{xyy}	-13.7476317
β_{yyy}	-161.8470719
β_{zxx}	0.0600745
β_{xyz}	0.1220257
β_{zyy}	-0.6719205
β_{xzz}	0.4894769
β_{yzz}	0.0155964
β_{zzz}	-0.0025623
β_{total}	1.1070
μ_x	0.4960665
μ_y	0.1145269
μ_z	0.0019529
μ	0.5091

V. CONCLUSION

In this work, the SQM force field method based on DFT calculations at the B3LYP/6-311+G** level have been carried out to analyze the vibrational frequencies of 1-Naphtol . Refinement of the scaling factors applied in this study achieved a weighted RMS deviation of 9 cm^{-1} between the experimental and scaled frequencies. This close agreement established between the experimental and scaled frequencies obtained using large basis set (6-311+G**) calculations has proved to be more reliable and accurate than the calculations using lower basis sets. The first-order hyperpolarizability (β_{ijk}) of the novel molecular system of 1-Naphtol is calculated using 3-21 G (d,p) basis set based on finite field approach. The calculated first-order hyperpolarizability (β_{total}) of 1-Naphtol is 1.1070×10^{-30} esu, which is nearly seven times that of urea (0.1947×10^{-30} esu).

ACKNOWLEDGMENT

The authors are thankful to the Sophisticated Analytical Instrumentation Facility (SAIF), IIT Madras, Chennai, for spectral measurements.

REFERENCES

[1] B.A. Hess Jr., J. Schaad, P. Carsky, R. Zahradnik, Chem. Rev. 86 (1986) 709.

[2] P. Pulay, X. Zhou, G. Fogarasi, in: R. Fausto (Ed.), NATO ASI Series, vol. C406, Kluwer, Dordrecht, 1993.

[3] C.E. Blom, C. Altona, Mol. Phys. 31 (1976) 1377.

[4] P. Pulay, G. Fogarasi, G. Pongor, J.E. Boggs, A. Vargha, J. Am. Chem. Soc. 105 (1983) 7037.

[5] G. Fogarasi, P. Pulay, in: J.R. Durig (Ed.), Vibrational Spectra and Structure, vol. 14, Elsevier, Amsterdam, 1985.

[6] G. Fogarasi, Spectrochim. Acta 53A (1997) 1211.

[7] G. Pongor, P. Pulay, G. Fogarasi, J.E. Boggs, J. Am. Chem. Soc. 106 (1984) 2765.

[8] G.R. De Mare, Y.N. Panchenko, C.W. Bock, J. Phys. Chem. 98 (1994) 1416.

[9] Y. Yamakita, M. Tasumi, J. Phys. Chem. 99 (1995) 8524.

[10] M.J. Frisch, G.W. Trucks, H.B. Schlega, G.E. Scuseria, M.A. Robb, J.R. Cheesman, V.G. Zakrzewski, J.A. Montgomery Jr., R.E. Stratmann, J.C. Burant, S. Dapprich, J.M. Millam, A.D. Daniels, K.N. Kudin, M.C. Strain, O. Farkas, J. Tomasi, V. Barone, M. Cossi, R. Cammi, B. Mennucci, C. Pomelli, C. Adamo, S. Clifford, J. Ochterski, G.A. Petersson, P.Y. Ayala, Q. Cui, K. Morokuma, N. Roga, P. Salvador, J.J. Dannenberg, D.K. Malick, A.D. Rabuck, K. Rahavachari, J.B. Foresman, J. Cioslowski, J.V. Ortiz, A.G. Baboul, B.B. Stefanov, G. Liu, A. Liashenko, P. Piskorz, I. Komaromi, R. Gomperts, R.L. Martin, D.J. Fox, T. Keith, M.A. Al-Laham, C.Y. Penng, A. Nanayakkara, M. Challa-Combe, P.M.W. Gill, B. Johnson, W. Chen, M.W. Wong, J.L. Andres, C. Gonzalez, M. Head-Gordon, E.S. Replogle and J.A. Pople, Gaussian 98, Revision A 11.4, Gaussian Inc., Pittsburgh, PA (2002).

[11] A.D. Becke, J.Chem. Phys.98 (1993) 5648

[12] C. Lee, W.Yang, R.G. Parr, Phys. Rev. B.37 (1998) 785.

[13] P. Pulary, G. Fogarasi, G. Pongor, J.E. Boggs, A. Vargha, J.Am. Chem. Soc. 105 (1983) 7037.

[14] G. Rauhut, P. Pulay, J. Phys. Chem.99 (1995) 3093.

[15] G. Fogarasi and P. Pulay In: J.R. Durig, Editor, Vibrational Spectra and Structure vol. 14, Elsevier, Amsterdam (1985), p. 125 (Chapter 3).

[16] G. Fogarasi, X. Xhov, P.W. Taylor and P. Pulay, J. Am. Chem. Soc. 114 (1992), p. 8191.

[17] T. Sundius. J.Mol. Struct. 218 (1990) 321.

[18] (a) T. Sundius, Vib. Spectrosc. 29 (2002) 89-95.
(b) MOLVIB (v.7.0), Calculation of harmonic force fields and vibrational modes of molecules, QCPE Program No. 807, 2002.

[19] P.L. Polavarapu, J. Phys. Chem. 94 (1990) 8106.

[20] G. Keresztury, S. Holly, J. Varga, G. Besenyei, A.V. Wang, J.R. Durig, Spectrochim. Acta 49A (1993) 2007.

[21] G. Keresztury, in: J.M. Chalmers and P.R. Griffiths(Eds), Handbook of Vibrational Spectroscopy vol.1, John Wiley & Sons Ltd. (2002), p. 71.

[22] A.D. Becke, J.Chem. Phys.98 (1993) 5648.

[23] H.D. Cohen, C.C.J. Roothan, J. Chem. Phys. 435 (1965) S34.

[24] D.N. Sathyanarayana, Vibrational Spectroscopy—Theory and Applications, second ed., New Age International (P) Limited Publishers, New Delhi, 2004.

[25] George Socrates, Infrared and Raman Characteristic Group Frequencies -Tables and Charts (third ed.), John Wiley & Sons, Chichester (2001).

[26] V. Krishna kumar, R. John Xavier, Indian J. Pure Appl. Phys. 41 (2003) 95.

[27] D.A. Kleinman, Phys. Rev. 126 (1962) 1977

[28] B. Lakshmaiah, G. Ramana Rao, J. Raman Spectrosc. 20 (1989) 439.

[29] G.Raja,K.Saravanan and S.Sivakumar,Int. J. of Curr. Res, 3 (2010) 46.